Solid-State Electronics Vol. 32, No. 12, pp. 1467–1471, 1989
Printed in Great Britain.

0038-1101/89 $3.00 + 0.00

INVERTED BISTABILITY IN THE CURRENT-VOLTAGE CHARACTERISTICS OF A RESONANT TUNNELING DEVICE

M. L. Leadbeater*, L. Eaves*, M. Henini*, O. H. Hughes*, G. Hill° and M. A. Pate°

*Department of Physics, University of Nottingham, Nottingham NG7 2RD, U.K.
°Department of Electrical and Electronic Engineering, University of Sheffield, Sheffield S1 3JD, U.K.

ABSTRACT

The current-voltage characteristics of an asymmetric double barrier resonant tunneling device show a butterfly-shaped hysteresis loop in which, for a range of voltage, the off-resonant current exceeds the resonant current. This "inverted bistability" is due to the effects of space charge buildup in the quantum well. Magnetoquantum oscillations in the tunnel current with $\underline{B} \| \underline{J}$ are used to investigate the distribution of charge within the device and the intersubband scattering processes which control the charge buildup.

KEYWORDS

Resonant tunneling; intrinsic bistability; intersubband scattering; sequential tunneling.

The buildup of electronic space charge in the quantum well of double barrier devices when resonant tunneling occurs is well established (Goldman, Tsui and Cunningham, 1987; Payling and co-workers, 1988; Young and co-workers, 1988). In structures with tunnel barriers of different thicknesses (Alves and co-workers, 1988) or potential barrier heights (Zaslavsky and co-workers, 1988) this charge buildup is enhanced and can lead to an intrinsic bistability effect in the current-voltage characteristics.

In this paper, we report magnetotransport studies of an intrinsic bistability effect in a resonant tunneling device for which the current-voltage characteristics I(V) show a "butterfly" shaped hysteresis loop. This bistability effect is shown to arise from an enhancement of the space charge buildup due to intersubband scattering processes. These are modulated by high magnetic fields leading to magneto-oscillations in the voltage width of the bistable region. The effect is observed in a double barrier structure in which two $Al_{0.4}Ga_{0.6}As$ barriers of thicknesses 5.7 and 14.1 nm enclose a quantum well of thickness 5.9 nm. The device was grown by molecular beam epitaxy. The layers, in order of growth from the n^+ GaAs substrate, were (i) a 2 μm thick buffer layer of GaAs doped with Si to n = 2 x 10^{18} cm^{-3}; (ii) a 51 nm thick layer of GaAs, n = 1 x 10^{17} cm^{-3}; (iii) a 51 nm layer of GaAs, n = 1 x 10^{16} cm^{-3}; (iv) a 3.4 nm undoped GaAs spacer layer; (v) a 5.7 nm undoped barrier of (AlGa)As, [Al] = 0.4; (vi) a 5.9 nm undoped GaAs well; (vii) a 14.1 nm undoped barrier of (AlGa)As, [Al] = 0.4; (viii) a 3.4 nm undoped GaAs spacer layer; (ix) a 51 nm layer of GaAs, n = 1 x 10^{16} cm^{-3}; (x) a 51 nm layer of GaAs, n = 1 x 10^{17} cm^{-3}; (xi) a 0.5 μm thick top contact layer of GaAs, n = 2 x 10^{18} cm^{-3}. Mesas of 100 and 200 μm diameter were etched and Au/Ge ohmic contacts made to the top and bottom layers of the devices.

The upper band diagram in Fig. 1 shows the variation of electron potential across the device under an applied voltage, V. The application of a voltage produces a quasi-two-dimensional electron gas (2DEG) and an accumulation layer in the lightly doped region adjacent to the emitter barrier. Electrons are continually removed from the accumulation layer by tunneling. The relatively low current passed by the device ensures that conduction electrons arriving from the heavily doped n^+ layer thermalize in the accumulation layer before tunneling through the emitter barrier. At low temperatures the 2DEG is degenerate. The two-dimensional nature of the emitter state is confirmed by the angular dependence of the magnetoquantum oscillations in the tunnel current. Resonant tunneling occurs when the energy of the quasi-bound state in the accumulation layer coincides with either of the quasi-bound states of the well (Thomas and co-workers, 1989). Because of the finite, but narrow, widths of these states, the tunnel rate from the emitter into the well (and hence the current) is a sharply-peaked function of the voltage drop V_e across the emitter barrier.

The current-voltage characteristics of the device are shown in Fig. 1 for a range of temperatures. We define forward bias as the arrangement in which the top contact, layer (xi), is biased positive so electrons first encounter the thinner of the two barriers. The voltage range corresponds to resonant tunneling into the upper bound state of the quantum well E_2 as shown schematically in the upper band diagram in Fig. 1. Because of the thick barriers in this device, resonant tunneling into the lower bound state E_1 can only be detected using A.C. measurements. In reverse bias, shown in Fig. 1(b), the resonant peak in the current for tunneling into E_2 is very weak (I = 60 nA at the peak) and spread over a relatively narrow range

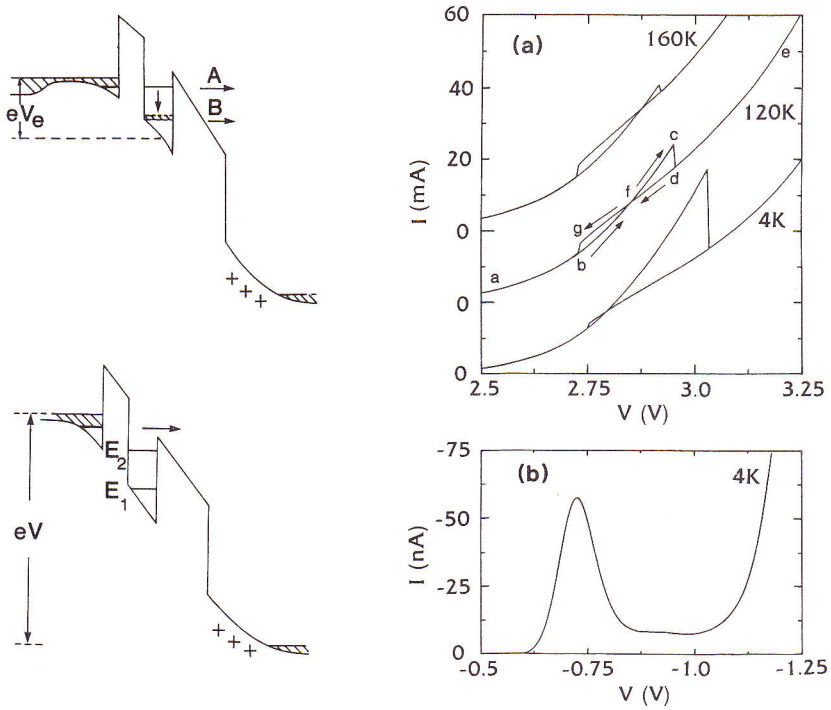

Fig. 1 Current-voltage characteristics of a 100 μm diameter mesa of the asymmetric double barrier structure. (a) forward bias at temperatures of 4, 120 and 160 K; (b) reverse bias at 4 K. The upper conduction band diagram illustrates the condition for resonant tunneling into the 2nd subband of the quantum well, with intersubband scattering and charge buildup in the lower subband. In the lower band diagram the device is off-resonance and electrons have energies greater than the height of the collector barrier.

of voltage ($\Delta V \sim 0.1$ V), with no bistability. In this case, charge buildup in the quantum well is small since electrons can easily tunnel out through the thinner barrier to the collector (Leadbeater and co-workers, 1988). The "butterfly" shaped hysteresis loop which we observe in forward bias (Fig. 1(a)) over the temperature range from 4 to 180 K is different in form from the intrinsic bistability effect reported by Alves and co-workers (1988) and Zaslavsky and co-workers (1988) although it also arises from space charge effects. The effect of space charge buildup is to spread the resonance over a wide range of V as shown schematically in Fig. 2. The change in V_e is small, the additional voltage being dropped almost entirely across the collector barrier and depletion layer. The low doping in the regions adjacent to the barriers increases the voltage drop in the depletion layer, magnifying the electrostatic feedback effect. In the intrinsic bistability effect reported previously, the value of the current on resonance always exceeds the off-resonant value (curve (ii) of Fig. 2). In the new device the effect of the space charge is even more pronounced (see curve (iii)) and causes an "inverted" bistability in which the off-resonant current in the range g to f exceeds the resonant value. At low temperatures resonant tunneling occurs over the voltage range from ~1.7 to 3.1 V.

Electrons tunneling resonantly into E_2 reach the collector either by tunneling directly through the collector barrier (process A) or by sequential tunneling (process B) - see the upper band diagram of Fig. 1. In the latter case, they undergo intersubband scattering into the lower bound state E_1 by the emission of longitudinal optic phonons and then tunnel out through the collector barrier (Eaves and co-workers, 1988; Hughes and co-workers, 1989). Estimates of the dwell times of electrons in E_1 and E_2 indicate that nearly all the current flowing through the device is due to process A. However, the dwell time of an electron in E_2 is sufficiently long compared to the intersubband scattering time ($\tau_i \sim 1$ ps, Bastard and Ferreira, 1989) to allow some electrons to undergo process B. Due to the low tunneling probability out of the lower bound state E_1, this leads to a significant buildup of electron sheet density (n_w) in the quantum well.

Both n_w and the sheet density in the emitter 2DEG, n_a, can be determined from the period of the magneto-oscillations in the tunnel current and differential capacitance when a magnetic field is applied, $\underline{B} \| \underline{J}$ (Leadbeater and co-workers, 1989). Briefly, the series of magneto-oscillations corresponding to each 2DEG arises from the passage of Landau levels through the respective quasi-Fermi levels. This modulates the charge densities, affecting the distribution of electric potential and hence the tunnel current and capacitance. Each series of oscillations is periodic in 1/B and the inverse period $\beta = [\Delta(1/B)]^{-1}$ gives the sheet densities $n_{a,w} = 2e\beta_{a,w}/h$. Typical series of magneto-oscillations at several fixed biases are shown in Fig. 3(a). Curves (i) and (iv) at biases below (1.4 V) and above (3.3 V) resonance respectively show only one series of magnetoquantum oscillations. This is attributed to the charge in the emitter 2DEG. The rapid

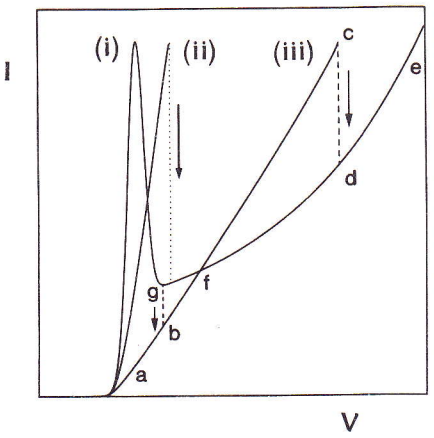

Fig. 2 Schematic diagram illustrating the effects of space charge buildup in the well on the current-voltage characteristics of a double-barrier device. (i) no charge in well, (ii) intrinsic bistability due to space charge buildup, (iii) large charge buildup leading to a region of inverted bistability.

oscillations apparent in trace (iii) at 2.5 V will be discussed below. Curve (ii) for a bias of 1.9 V clearly shows two series of oscillations. The existence of clear magneto-oscillations due to the 2DEG associated with the quasi-bound state E_1 of the well requires that it has a well-defined quasi-Fermi energy which is different from that in the emitter. These oscillations are observed down to magnetic fields ~0.8 T. This means that the electron temperature is low ($kT_e \ll \hbar\omega_c$) and therefore the electrons must undergo energy relaxation in the well. Following the intersubband transition, and possibly further emission of LO phonons, this occurs via deformation potential scattering on a timescale $\lesssim$ 1 ns (Sheard, 1989). This is shorter than the mean time for an electron to tunnel from the bound state E_1 through the thick collector barrier (> 10 ns). At these sheet densities electron-electron scattering is expected to be rapid and to produce a thermalized (Maxwellian) electron energy distribution (with some effective temperature much higher than the lattice temperature) on a timescale < 100 fs (Deveaud and co-workers, 1988; Knox, Chemla and Livescu, 1988). However, this process can only redistribute energy between electrons and cannot provide the overall energy relaxation required to produce the cold Fermi-Dirac distribution necessary for the observation of well-defined magnetoquantum oscillations. This must occur on the much longer timescale of deformation potential scattering. Note that the observation of a degenerate electron gas in the lower subband when electrons are tunneling into the upper subband is a clear demonstration of sequential tunneling. Since both the tunneling rate from E_2 and the intersubband scattering rate are much faster than the energy relaxation rate, the electron density in E_2 is low and non-degenerate and does not give rise to a series of magneto-oscillations. If we were to assign the measured n_w to the upper subband this would give rise to a current density $J = n_w e/\tau \sim 10^9$ Am^{-2}, three orders of magnitude higher than observed. The much slower tunneling rate from the lower subband is consistent with the measured current density.

The variations of n_a and n_w with applied bias are shown in Fig. 3(b). As the device comes on to resonance n_a remains approximately constant and charge builds up in the quantum well. At biases above about 2.5 V, the electron sheet density in the well exceeds that in the accumulation layer. This is in contrast to previous work (Leadbeater and co-workers, 1989) where the charge density in the well was always less than that in the accumulation layer. In that case tunneling was taking place into the lower subband and its energy level was essentially coincident with that of the emitter 2DEG, hence its Fermi energy (and therefore number density) could not exceed that in the emitter. For the resonance described here, although the charge is building up in the lower subband this is due to intersubband scattering and the energy level is considerably below that of the quasi-bound state of the emitter 2DEG. Hence the quasi-Fermi energy in the well can exceed that in the emitter.

If the voltage is increased beyond the peak of the resonance, the current drops abruptly (c → d in Fig. 1(a) and Fig. 2), as does the electron sheet density in the well, n_w. This is compensated by an increase in n_a so as to maintain the same voltage drop across the device as seen in Fig. 3(b). Note that this switch occurs at lower bias in the presence of a magnetic field as discussed below. The device remains in the off-resonant state when the voltage is increased up to and beyond point e or reduced back to point g. From the sheet charges in the accumulation layer and quantum well obtained from the magnetoquantum oscillations, we can use Gauss's Law to determine the potential distribution across the device over a wide range of operating conditions. Such an analysis shows that over the voltage range from e to g, electrons are injected through to the collector at energies well above the height of the collector barrier, as shown in the lower band diagram of Fig. 1. Therefore they only encounter one tunnel barrier.

When the voltage is further reduced, the device makes the transition back to the resonant tunneling state (g → b). In state b, n_w is significantly larger and n_a significantly smaller than in state g, so that the top of the collector barrier is at a considerably higher potential energy, as can be seen by comparing the two band profile diagrams in Fig. 1. Because of the

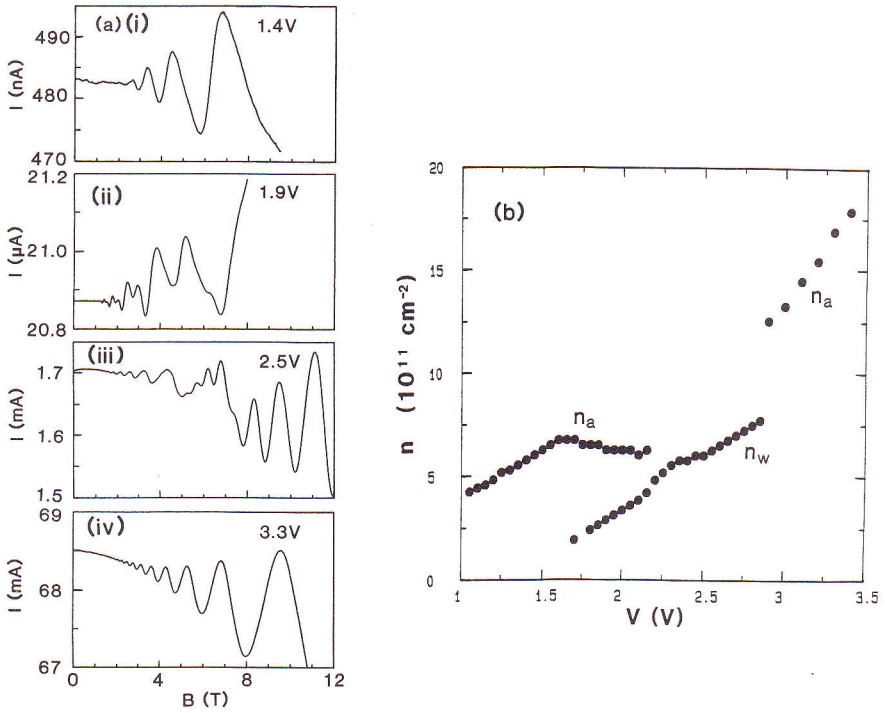

Fig. 3(a) Typical magnetoquantum oscillations in the tunnel current with $\underline{B} \| \underline{J}$ at 4 K. (i) 1.4 V (ii) 1.9 V, (iii) 2.5 V and (iv) 3.3 V.
(b) Variation with applied bias of the 2DEG sheet density in the accumulation layer, n_a, and the quantum well, n_w.

increased height of the collector barrier in state b, the lifetime of the E_2 resonance is sufficiently long to allow intersubband scattering of electrons into E_1, from which they tunnel into the collector with low transmission rate. Over the range g-f, the non-resonant current exceeds the resonant current at the onset (b-f) of the resonant peak. The large non-resonant current arises because the electrons have to tunnel through only the emitter barrier, across which the voltage drop is larger than in the resonant case.

The analysis is supported by the temperature dependence of the bistability, shown in Fig. 1(a). The non-resonant current is more temperature-dependent than the resonant current due to increasing contributions from phonon-assisted processes and energetic thermal electrons in the high energy tail of the distribution function of the emitter layer. Hence as the temperature is increased, the non-resonant current exceeds the resonant current over a wider voltage range, giving rise to a more pronounced inverted bistability. As the temperature increases, the charge buildup decreases, leading to a shift of the peak to lower bias, as seen in Fig. 1(a).

The strong influence of a quantising magnetic field $\underline{B} \| \underline{J}$ on the current-voltage characteristics can be seen in Fig. 4(a), which shows a series of up-voltage sweeps at different magnetic fields. The width of the bistable region decreases at low fields and the voltage position of the resonant peak V_p oscillates as shown in Fig. 4(b). We attribute this to a modulation of the intersubband scattering rate $1/\tau_i$ due to the formation of Landau levels in the quantum well. The effect of a magnetic field on the intersubband scattering rate can also be seen in the I(B) curve of Fig. 3(a) trace (iii) at 2.5 V. The scattering rate will be a maximum when

$$E_2 - E_1 - \hbar\omega_{LO} = j\hbar\omega_c = \hbar e\beta/m^* \qquad (1)$$

where j is an integer, $\hbar\omega_{LO}$ the LO phonon energy and $\hbar\omega_c$ is the cyclotron energy. The modulation of τ_i by the magnetic field alters the charge in the well, n_w. This changes the distribution of electric potential within the device and the voltage position of the peak. The tunneling probabilities are also altered, which in turn affect the tunnel current. Since the current is dominated by electrons tunneling directly from E_2 (process A in Fig. 1), the magnetic-field induced oscillations in the tunnel current must be primarily due to the electrostatic effect of the modulation of the charge in E_1. The high-field magneto-oscillations in Fig. 3(a) (iii) have a frequency $\beta \sim 70$ T, which corresponds to an energy $e\beta\hbar/m^* \sim 110$ meV. This is much higher than the Fermi energies of the 2DEGs in the well and accumulation layer. Since the observation of this series does not depend on Landau levels passing through a well-defined Fermi level but just on the intersubband energy separation, this series of oscillations can be observed at much higher temperatures (> 100 K) than the accumulation layer and well series. Note that trace (iv) of Fig. 3(a), at a bias (3.3 V) beyond the resonant peak shows only one series of magnetoquantum oscillations. No intersubband scattering is observed since the electrons are injected into the well region at energies higher than the collector barrier. The

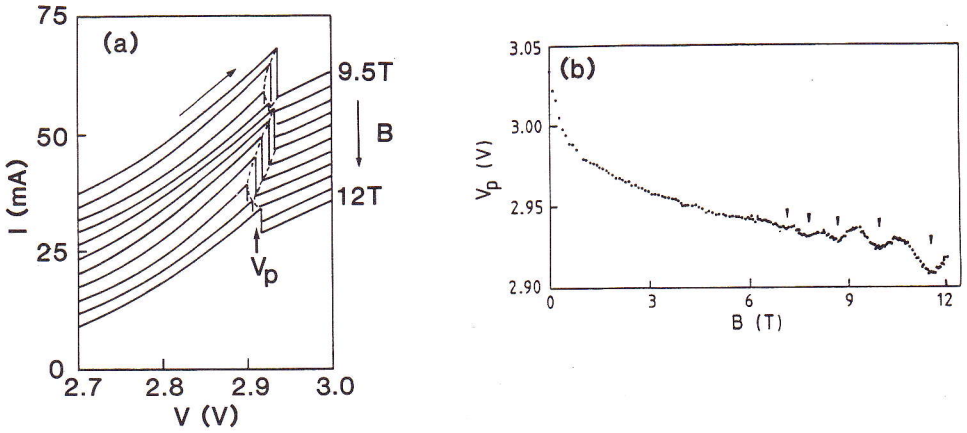

Fig. 4(a) Effect of a magnetic field B‖J on the current-voltage characteristics (increasing V) at T = 4.2 K. The vertical axis corresponds to the current at B = 12 T and the other curves are displaced vertically for clarity.
(b) Variation with magnetic field of the voltage V_p at the resonant peak. The magneto-oscillations given by equation (1) are indicated by arrows.

transit time across the well is much shorter than that for LO phonon emission and no charge builds up in the lower subband. Similarly, in reverse bias, the narrow width of the collector barrier reduces the electron dwell time and the intersubband scattering series is not observed. The variation in V_p with field shown in Fig. 4(b) is periodic in 1/B as expected from equation (1), with a β-value close to that shown in Fig. 3(a) (iii). Taking $\hbar\omega_{LO}$ = 36 meV, the periodicity obtained gives a value of 140 meV for the intersubband energy separation, which is close to that expected for a well of this thickness under an applied bias.

To summarise, we have observed a new type of bistability effect in double barrier resonant tunneling devices based on n-type GaAs/(AlGa)As in which the off-resonant current exceeds the resonant current over a range of voltage. This arises from the enhancement of space charge buildup in the quantum well due to intersubband scattering. Magnetoquantum oscillations in the tunnel current are attributed to a degenerate gas of electrons in the quantum well which thermalize to the lattice temperature. Modulation of the intersubband scattering rate by a quantizing magnetic field leads to a periodic oscillation in the voltage width of the bistable region.

ACKNOWLEDGEMENTS

We are grateful to Dr. P. E. Simmonds of the University of Wollongong, Australia, for useful discussions. This work is supported by SERC (UK).

REFERENCES

Alves, E. S., L. Eaves, M. Henini, O. H. Hughes, M. L. Leadbeater, F. W. Sheard, G. A. Toombs, G. Hill and M. A. Pate (1988). *Electronics Letters* 24, 1190-1191.
Bastard, G. and R. Ferreira (1989). *Proc. Int. Conf. on Quantum Wells for Optoelectronics*, Salt Lake City.
Deveaud, B., J. Shah, T. C. Damen, A. C. Gossard and P. Lugli (1988). *Solid-State Electronics* 31, 435-438.
Eaves, L, G. A. Toombs, F. W. Sheard, C. A. Payling, M. L. Leadbeater, E. S. Alves, T. J. Foster, P. E. Simmonds, M. Henini, O. H. Hughes, J. C. Portal, G. Hill and M. A. Pate (1988). *Appl. Phys. Lett.* 52, 212-214.
Goldman, V. J., D. C. Tsui and J. E. Cunningham (1987). *Phys. Rev. B* 35, 9387-9390.
Hughes, O. H., M. Henini, E. S. Alves, L. Eaves, M. L. Leadbeater, F. W. Sheard, G. A. Toombs, G. Hill, M. A. Pate, J. C. Portal and A. Celeste (1989). *J. Cryst. Growth* 95, 352-356.
Knox, W. H., D. S. Chemla and G. Livescu (1988). *Solid-State Electronics* 31, 425-430.
Leadbeater, M. L., E. S. Alves, L. Eaves, M. Henini, O. H. Hughes, F. W. Sheard and G. A. Toombs (1988). *Semicond. Sci. Technol.* 3, 1060-1062.
Leadbeater, M. L., E. S. Alves, L. Eaves, M. Henini, O. H. Hughes, F. W. Sheard and G. A. Toombs (1989). *Superlattices and Microstructures* 6, 59-62.
Sheard, F. W. (1989). 3rd Int. Conf. Phonon Physics, Heidelberg 1989.
Thomas, D., F. Chevoir, P. Bois, E. Barbier, Y. Guldner and J. P. Vieren (1989). *Superlattices and Microstructures* 5, 219-221.
Young, J. F., B. M. Wood, G. C. Aers, R. L. S. Devine, H. C. Liu, D. Landheer, M. Buchanan, A. J. SpringThorpe and P. Mandeville (1988). *Phys. Rev. Lett.* 60, 2085-2088.
Zaslavsky, A., V. J. Goldman and D. C. Tsui (1988). *Appl. Phys. Lett.* 53, 1408-1410.